Acta Biomaterialia 150 (2022) 199–210

Contents lists available at ScienceDirect

Acta Biomaterialia

journal homepage: www.elsevier.com/locate/actbio

Full length article

A double crosslinking adhesion mechanism for developing tough hydrogel adhesives

Joonsu Han[a], Jihoon Park[a], Rimsha Bhatta[a], Yusheng Liu[a], Yang Bo[a], Jingyi Zhou[a], Hua Wang[a,b,c,d,e,f,g,*]

[a] Department of Materials Science and Engineering, University of Illinois at Urbana-Champaign, Urbana, IL 61801, United States
[b] Cancer Center at Illinois (CCIL), Urbana, IL 61801, United States
[c] Department of Bioengineering, University of Illinois at Urbana-Champaign, Urbana, IL 61801, United States
[d] Carle College of Medicine, University of Illinois at Urbana-Champaign, Urbana, IL 61801, United States
[e] Beckman Institute for Advanced Science and Technology, University of Illinois at Urbana-Champaign, Urbana, IL 61801, United States
[f] Materials Research Laboratory, University of Illinois at Urbana-Champaign, Urbana, IL 61801, United States
[g] Institute for Genomic Biology, University of Illinois at Urbana-Champaign, Urbana, IL 61801, United States

ARTICLE INFO

Article history:
Received 18 March 2022
Revised 11 July 2022
Accepted 15 July 2022
Available online 20 July 2022

Keywords:
Tough gel
Bioadhesive
Hydrogel
Tissue adhesive
Drug depot

ABSTRACT

Tough hydrogel adhesives that consist of a robust gel network and can strongly adhere to wet tissues have shown great promise as the next generation of bioadhesives. While a variety of chemistries can be utilized to construct the tough gel network, the covalent conjugation methods for tissue adhesion are still limited. Here we report, for the first time, the use of side product-free amine-thiolactone chemistry which initiates a double crosslinking adhesion mechanism to develop tough gel adhesives. Thiolactone groups can conjugate with tissue-surface amines via a ring-opening reaction. The resultant thiol end groups can be further crosslinked into disulfide linkages, enabling the formation of a robust and stable adhesion layer. The thiolactone-bearing tough hydrogel composed of methacrylate-modified gelatin, acrylic acid, and thiolacone acrylamide exhibited good biocompatibility and mechanical properties, and strong adhesion to various types of engineering solids and tissues. We also demonstrated its ability to function as a tissue sealant and drug depot. The novel adhesion mechanism will diversify future design of bioadhesives for hemostasis, drug delivery, tissue repair, and other applications.

Statement of significance

Tough hydrogel adhesives with excellent tissue-adhesive and mechanical properties have demonstrated tremendous promise for hemostasis, tissue repair, and drug delivery applications. However, the covalent chemistry for tissue adhesion has been limited, which narrows the choice of materials for the design of bioadhesives and may pose a safety concern. Here, for the first time, we report the use of side product-free amine-thiolactone chemistry, which involves a double crosslinking adhesion mechanism, for developing tough hydrogel adhesives. We demonstrate that thiolactone-bearing tough hydrogels exhibit favorable biocompatibility and mechanical properties, and superior adhesion to both engineering solids and tissues. Our new adhesion technology will greatly facilitate future development of advanced bioadhesives for numerous biomedical applications.

1. Introduction

Bioadhesives that can strongly adhere to wet tissues have shown tremendous promise for hemostasis, tissue repair, drug delivery, and other applications [1–4]. The design of bioadhesives was initially inspired by nature where living organisms (barnacle, slug, gecko, abalone, worms, etc.) secrete molecules and biopolymers onto the residing surface to form an adhesion layer [5–10]. The adhesion layer was often viscous and capable of improving the retention of the body on the residing surface, but suffered from low adhesion energy and poor mechanical strength. The need of tougher and stronger adhesives motivated more in-depth understanding of adhesion mechanisms, which later shed light on the critical roles of both the adhesion layer and bulk gel network in generating a strong and stable adhesion [3,6]. The adhesion layer estab-

* Corresponding author.
E-mail address: huawang3@illinois.edu (H. Wang).

https://doi.org/10.1016/j.actbio.2022.07.028
1742-7061/

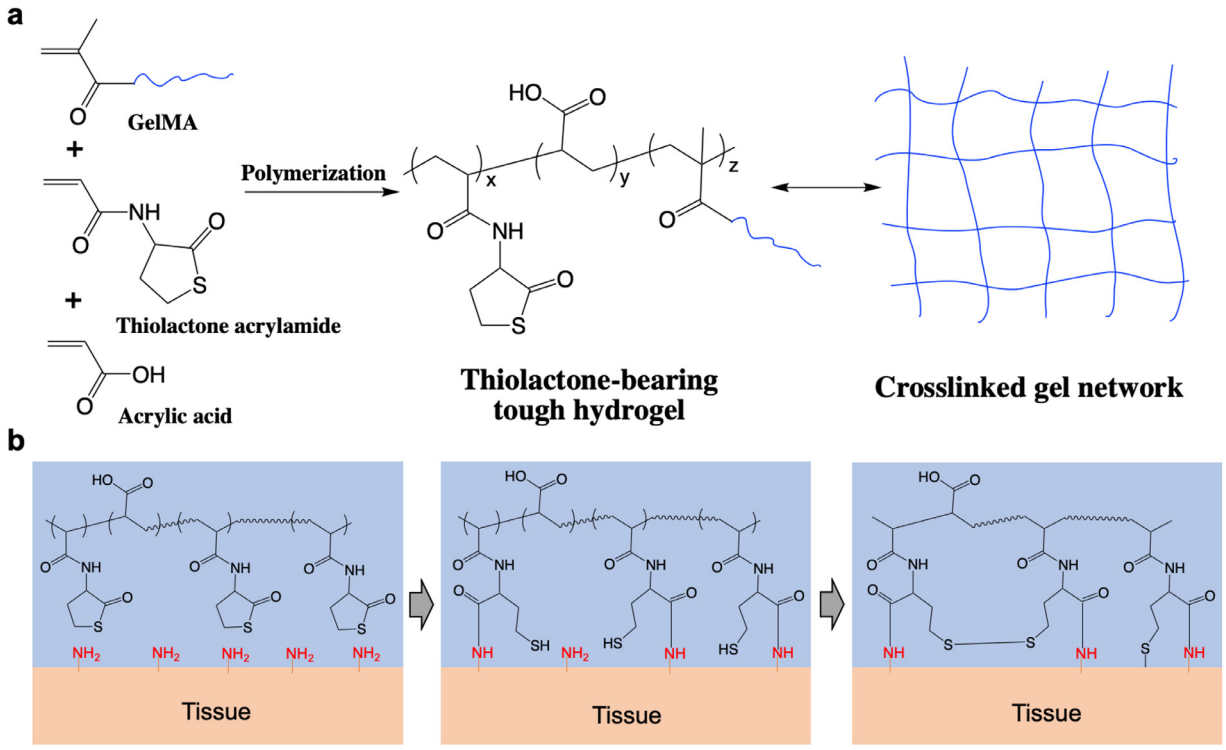

Fig. 1. (a) Schematic illustration for the synthesis of thiolactone-bearing tough hydrogels via co-polymerization of GelMA, thiolactone acrylamide, and acrylic acid in the presence of α-ketoglutaric acid and ultraviolet light. (b) Schematic illustration for the adhesion of thiolactone-bearing tough hydrogels to wet tissues via the ring-opening reaction between amine and thiolactone groups and subsequent crosslinking of the resultant thiol groups.

lishes connection between tissues and adhesives, while the bulk gel network provides mechanical strength and enables the dissipation of energy from the adhesion layer [3,6,11]. Various types of covalently-crosslinked, ionically-crosslinked, and hybrid gel networks have been successfully used to construct tough hydrogels [12–14]. For example, the combination of calcium ion-crosslinked alginate and covalently crosslinked alginate was able to form a tough hydrogel with superior mechanical strength [3,15]. For the adhesion layer, hydrogen bond, van der Waals force, and hydrophobic interaction are the common types of interactions that bring tissues and adhesives together, partially due to the large library of molecules and polymers that can form these interactions [16–20]. However, these non-covalent interactions are still relatively weak to form a stable adhesion layer towards wet tissues, especially tissues that function in a highly mobile and mechanically-demanding environment (heart, muscles, joints, etc.) [21–24]. Also, the strength of these non-covalent interactions vary with the type of molecules and materials, requiring custom-design of the adhesion layer for each bioadhesive candidate.

Compared to non-covalent interactions, covalent linkages can significantly improve the stability of adhesion towards wet tissues and can be universally applied to different material systems [3,6]. Tissue surface contains amine (-NH_2), carboxyl (-COOH), and hydroxyl (-OH) groups that are originated from proteins, saccharides, metabolites, and extracellular matrix [25–28]. Among them, amines have been widely explored for the conjugation of *N*-hydroxysuccinimidyl (NHS)-bearing compounds [29–32]. Recently, amine-NHS chemistry was also successfully used to develop tough hydrogel adhesives [3,6]. In these designs, alginate- or gelatin-based tough hydrogels bearing carboxyl or NHS groups can react with amines on the surface of tissues to form an adhesion layer. The stable covalent linkage, together with the ability of tough gel network to dissipate energy from the adhesion layer, resulted in strong and robust adhesion [3,30]. However, the generation of NHS as a side product in this reaction, albeit neglected to some extent for in vitro and *ex vivo* studies, could pose a safety concern for in vivo applications. Nevertheless, amine-NHS reaction remains one of the most commonly used chemistries for forming covalent linkages with tissues to date [25,30,33–35]. These issues motivate the development of novel covalent adhesion mechanisms, especially those enabling stronger adhesion and avoiding the generation of side products, for diversifying the design of bioadhesives with optimal adhesive properties, biocompatibility, and mechanics.

Here we report the use of amine-thiolactone chemistry, which is free from any side product upon conjugation and enables a double crosslinking mechanism, for the design of tough hydrogel adhesives that can strongly adhere to wet tissues with high adhesion energy and mechanical strength (Fig. 1). Thiolactone-bearing tough hydrogels can be synthesized by copolymerizing thiolactone acrylamide, methacrylate-modified gelatin (GelMA), and acrylic acid via free radical polymerization (Fig. 1a). Upon contact with tissues, gels can adsorb water at the interface and expose thiolactone groups which can then conjugate with amines on the surface of tissues via a ring-opening reaction [36–38], resulting in the formation of thiol end groups without generating any side product. The resultant thiol groups can be further crosslinked into disulfide linkages to strengthen the adhesion layer (Fig. 1b). We show that thiolactone-bearing tough hydrogels exhibited high mechanical strength, great biocompatibility, and robust adhesion towards both engineering solids and wet tissues (porcine skin, small intestines, and liver). A variety of applications including hemostasis, drug delivery, and tissue repair can be envisioned with this type of tough gel adhesives [39–41]. The successful use of amine-thiolactone chemistry to induce stable and covalent adhesion of materials to tissues paves a new way for developing robust bioadhesives.

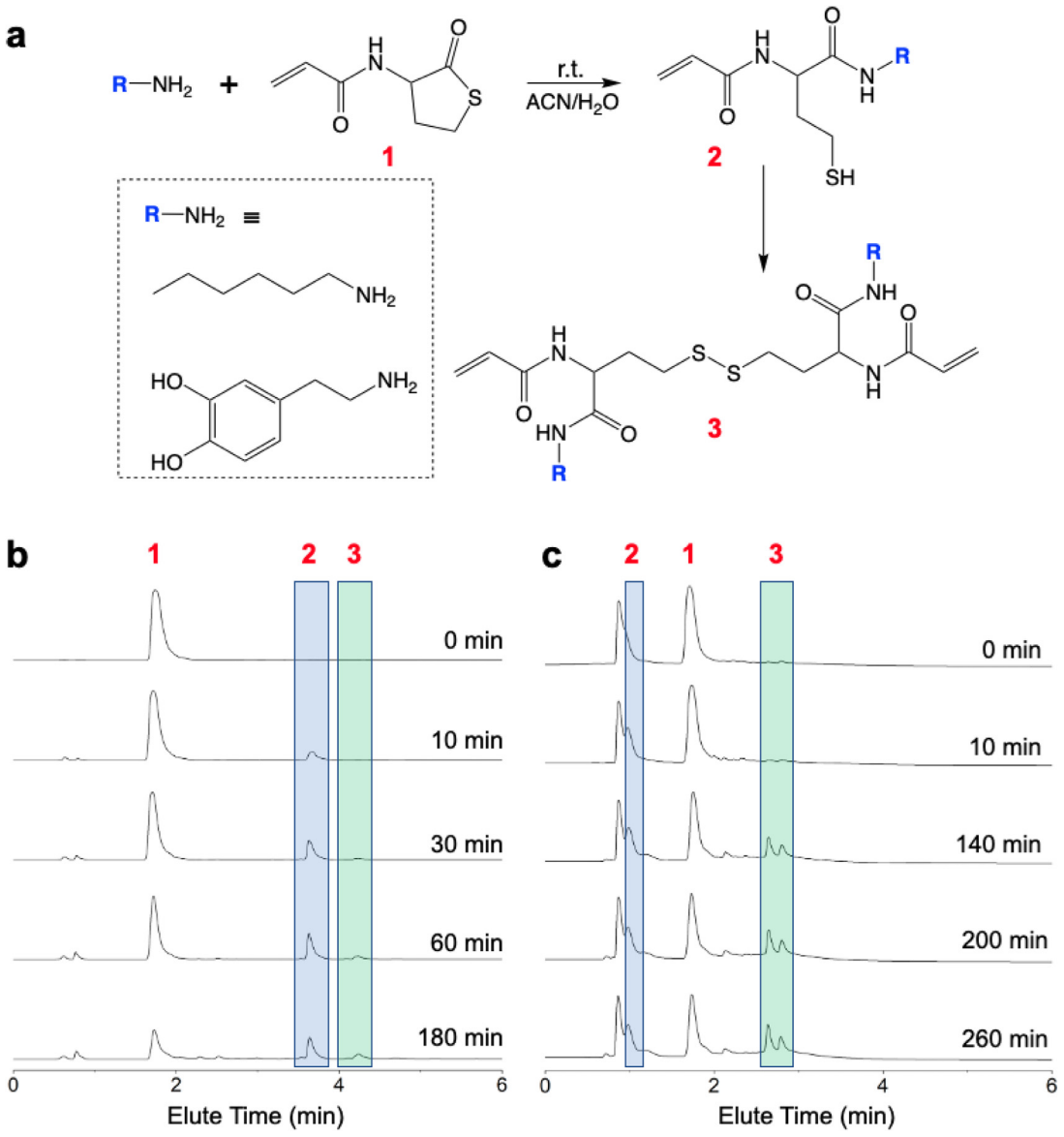

Fig. 2. Rapid reaction between thiolactone and amine groups. (a) Schematic illustration of the conjugation between amine and thiolactone groups and subsequent crosslinking of the formed thiols. Hexylamine and dopamine structures are shown. (b) HPLC profiles of the reaction mixture of hexylamine and thiolactone acrylamide at 0, 10, 30, 60, and 180 min post mixing. The peaks corresponding to the formed thiol-bearing compound 2 and disulfide-containing compound 3 are highlighted. Detection wavelength was set at 254 nm. (c) HPLC profiles of the reaction mixture of dopamine and thiolactone acrylamide at 0, 10, 140, 200, and 260 min post mixing. The peaks corresponding to the formed thiol-bearing compound 2 and disulfide-containing compound 3 are highlighted. Detection wavelength was set at 254 nm.

2. Methods

2.1. Materials

D,L-Homocysteine thiolactone hydrochloride, acryloyl chloride, triethylamine, acrylic acid, gelatin methacrylate(gelMA), acrylic acid *N*-hydroxysuccinimide ester, α-ketoglutaric acid, gelatin, and hexamethyldiamine (HMDA) were purchased from Sigma-Aldrich (St. Louis, MO, USA) and used without further purification. The engineering solid (polycarbonate) was purchased from Mcmaster Carr (Elmhurst, IL, USA). All porcine tissues for adhesion tests were purchased from Sierra for Medical Science (Whittier, CA, USA). Poly (methyl methacrylate) films with a thickness of 50 μm were purchased from VWR International (Radnor, PA, USA). Calcein AM and ethidium homodimer 1 were purchased from Thermofisher (Waltham, MA, USA). Primary antibodies used in this study, including fluorescein isothiocyanate (FITC)-conjugated anti-CD45 (Invitrogen), PE-conjugated anti-CD11b (Invitrogen), PE/Cy7-conjugated anti-CD11c (Invitrogen), Alexa Fluor 700-conjugated anti- Ly-6 G/Ly-6C (Invitrogen), PerCP/Cy5.5-conjugated anti-F4/80 (Invitrogen) were purchased from Thermo Fisher Scientific (Waltham, MA, USA). Fixable viability dye efluor780 was obtained from Thermo Fisher Scientific (Waltham, MA, USA). All antibodies were diluted according to the manufacturer's recommendations. Amine-Modified Microspheres and Alexa Fluor™ 660 C2 Maleimide were purchased from Thermo Fisher Scientific (Waltham, MA, USA). Small molecule compounds were run on the Agilent 1290/6140 ultra-high performance liquid chromatography/mass spectrometer or the Shimadzu high performance liquid chromatography. Proton and carbon nuclear magnetic resonance spectra were collected on the Varian U500 or VXR500 (500 MHz) spectrometer. Fluorescent images were taken with a EVOS microscope (Thermofisher, Waltham, MA, USA). Fluorescence measurement was conducted on a Biotek plate reader (BioTek Instruments, Winooski, VT, USA). Me-

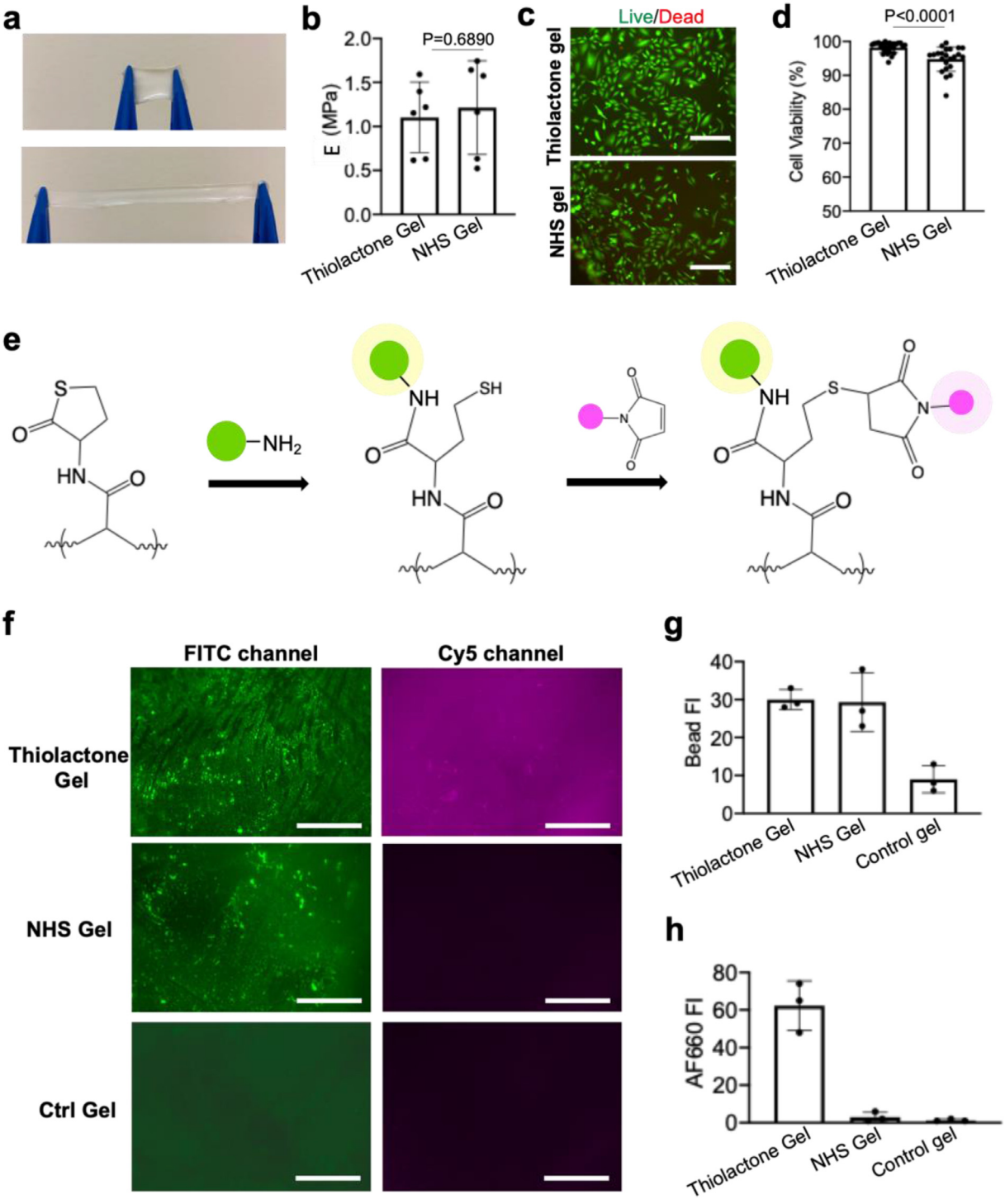

Fig. 3. Thiolactone-bearing gelatin hydrogels are mechanically tough, biocompatible, and reactive to amine-bearing surface. (a) Pictures illustrating the highly-stretchable thiolactone-bearing tough hydrogel (24 mm × 24 mm × 0.25 mm). (b) Elastic moduli of thiolactone- or NHS-bearing tough hydrogels. (c) Fluorescence images of 3T3-L1 fibroblasts cultured on thiolactone- or NHS-bearing tough hydrogels for 48 h. Live and dead cells were stained with Calcein AM and Ethidium Homodimer-1, respectively. Scale bar: 300 μm. (d) Quantification of 3T3-L1 viability after cultured on thiolactone- or NHS-bearing tough hydrogels for 48 h. (e) Schematic illustration of validation of the two-step adhesion mechanism. Gels were incubated with amine-modified microbeads (green fluorescent) for 30 min, and then incubated with Alexa Fluor 660 maleimide for 30 min. (f) Representative fluorescence images of gels under the FITC or Cy5 channel. Also shown are (g) Microbead fluorescence intensity and (h) Alexa Fluor 660 fluorescence intensity of gels, as measured on a plate reader. Scale bar: 300 μm for FITC channel / 750 μm for Cy5 channel All the numerical data are presented as mean ± SD ($0.01 < {}^{*}P \leq 0.05$; ${}^{**}P \leq 0.01$; ${}^{***}P \leq 0.001$). (For interpretation of the references to colour in this figure legend, the reader is referred to the web version of this article.)

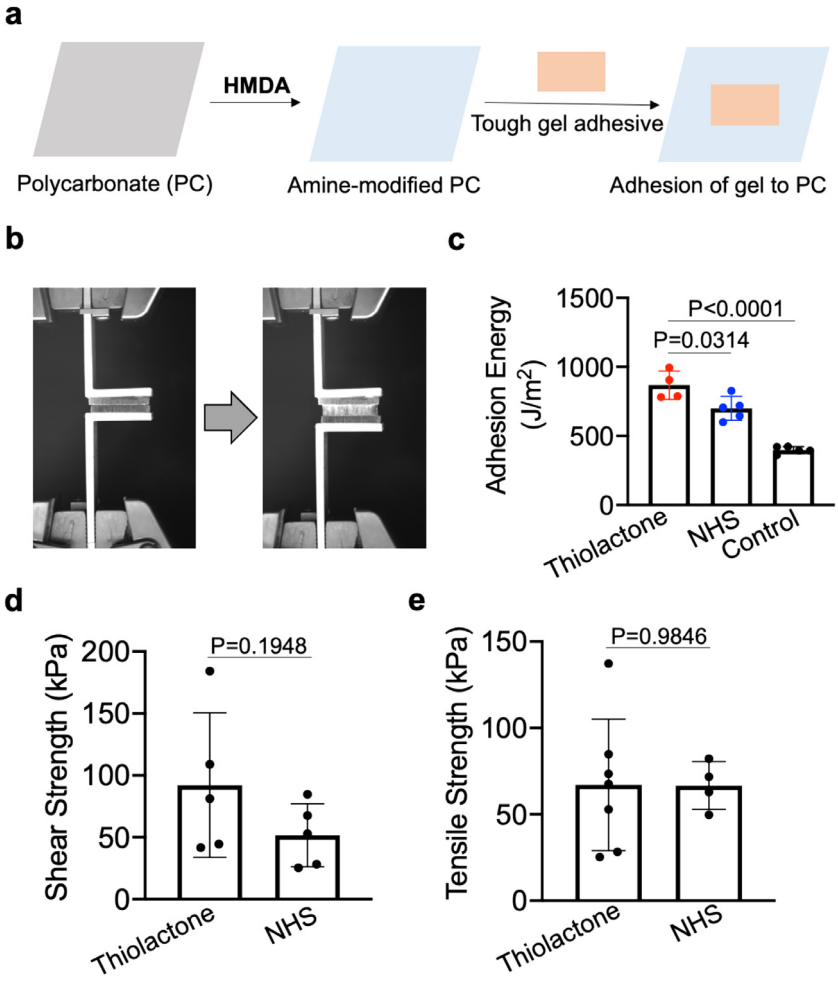

Fig. 4. Thiolactone-bearing tough hydrogels can rapidly and strongly adhere to amine-modified engineering solids. (a) Modification of polycarbonate (PC) substrates with amine groups and subsequent adhesion of thiolactone- or NHS-bearing tough hydrogels. (b) Pictures illustrating the peeling test of PC substrates adhered together by thiolactone-bearing tough hydrogels (24 × 24 × 0.25 mm in dimension), which showed the strong adhesion of gels to PC substrates. (c) Adhesion energy of thiolactone- or NHS-bearing tough hydrogels (24 × 24 × 0.25 mm). Thiolactone-bearing gels adhered to unmodified PC substrates were used as the control. (d) Shear strength of thiolactone- or NHS-bearing tough hydrogels (24 × 24 × 0.25 mm). (e) Tensile strength of thiolactone or NHS-bearing tough hydrogels (24 × 24 × 0.25 mm). All the numerical data are presented as mean ± SD ($0.01 < {}^{*}P \leq 0.05$; ${}^{**}P \leq 0.01$; ${}^{***}P \leq 0.001$). (For interpretation of the references to colour in this figure legend, the reader is referred to the web version of this article.)

chanical tests were performed with Criterion C43.104E (MTS, Eden Prairie, MN). FACS analyses were collected on Attune NxT flow cytometers and analyzed on FCS Express v6 and v7. Statistical testing was performed using GraphPad Prism v8.

2.2. Cell line and animals

3T3-L1 cell line was purchased from American Type Culture Collection (Manassas, VA, USA). Cells were cultured in DMEM containing 10% FBS, 100 units/mL Penicillin G and 100 μg/mL streptomycin at 37 °C in 5% CO_2 humidified air. Female C57BL/6 mice were purchased from Jackson Laboratory (Bar Harbor, ME, USA). Feed and water were available ad libitum. Artificial light was provided in a 12/12 hour cycle. All procedures involving animals were done in compliance with National Institutes of Health and Institutional guidelines with approval from the Institutional Animal Care and Use Committee at the University of Illinois at Urbana-Champaign.

2.3. Synthesis of thiolactone acrylamide

$_{D,L}$-Homocysteine thiolactone hydrochloride (10 mmol) was dissolved in methylene chloride, followed by the addition of acryloyl chloride (20 mmol). Triethylamine (25 mmol) in methylene chloride was added dropwise into the reaction mixture on ice bath. The reaction mixture was stirred for 24 h. The generated triethylamine hydrocloride salt was removed by washing the reaction mixture with deionized water for three times. The solvent was then removed under reduced pressure, and the solid crude product was further purified with silica column chromatography using ethyl acetate/hexane as the eluent. ^{1}H NMR (400 MHz, DMSO–d_6) δ 8.46 (d, J = 8.2 Hz, 1H), 6.29–6.16 (m, 1H), 6.18–6.06 (m, 1H), 5.72–5.61 (m, 1H), 4.68 (dt, J = 12.5, 7.4 Hz, 1H), 3.47–3.36 (m, 2H), 2.50–2.09 (m, 2H). ^{13}C NMR (126 MHz, DMSO–d_6) δ 205.69, 164.98, 131.13, 126.66, 58.47, 30.43, 27.05.

2.4. Thiolactone-amine chemistry validation

Thiolactone acrylamide (1.0 molar equiv.) and amine compounds (hexylamine or dopamine hydrochloride, 1.0 molar equiv.) were separately dissolved in 1 mL of acetonitrile/water (50%/50%, v/v). 100 μL of thiolactone acrylamide solution and 100 μL of amine compound solution were mixed to initiate the reaction. For the reaction between thiolactone acrylamide and dopamine hydrochloride, triethylamine (1.0 molar equiv.) was added. At selected

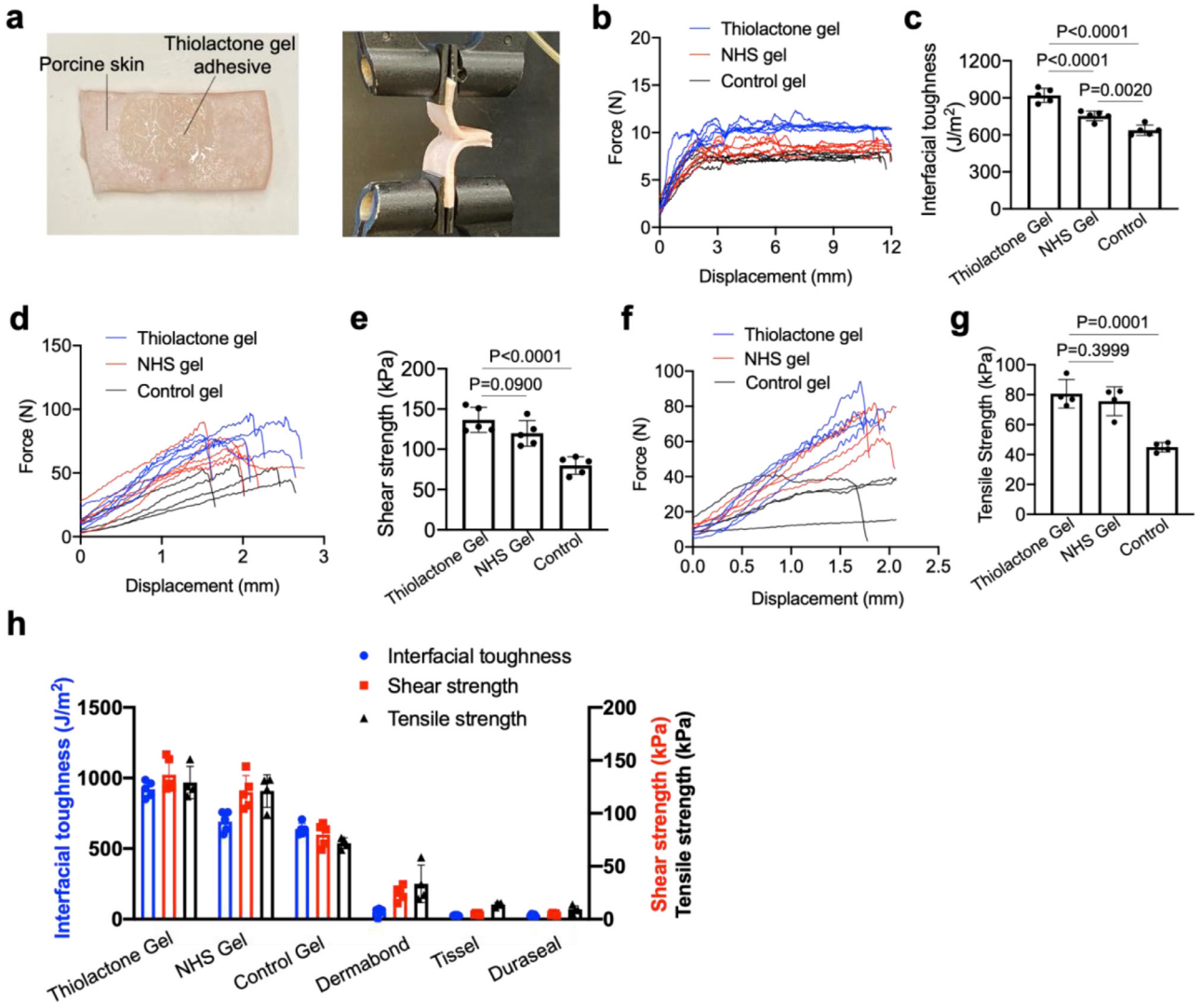

Fig. 5. Thiolactone-bearing tough hydrogels can rapidly and strongly adhere to porcine skin. (a) Pictures illustrating the adhesion of thiolactone-bearing tough hydrogels towards porcine skin and the peeling test. (b) Force-displacement profiles and (c) interfacial toughness of porcine skin adhered by thiolactone or NHS or control gels (24 × 24 × 0.25 mm), as determined via a peeling test. (d) Force-displacement profiles and (e) shear strength of porcine skin adhered by thiolactone or NHS or control gels (24 × 24 × 0.25 mm), as determined via a lap-shear test. (f) Force-displacement profiles and (g) tensile strength of porcine skin adhered by thiolactone or NHS or control gels (24 × 24 × 0.25 mm), as determined via a tensile test. (h) Comparison of the interfacial toughness, sheer strength, and tensile strength between different groups. All the numerical data are presented as mean ± SD ($0.01 < {}^{*}P \leq 0.05$; ${}^{**}P \leq 0.01$; ${}^{***}P \leq 0.001$). (For interpretation of the references to colour in this figure legend, the reader is referred to the web version of this article.)

time points, 5 μL of mixture solution was injected into HPLC for reaction monitoring.

2.5. Surface chemistry validation

Thiolactone-bearing gels, NHS-bearing gels, and control gels without any modification were prepared. Gels were placed in PBS in 48-well plates. After gels were fully swollen, Amine-Modified Microspheres (ex/em: 505/515 nm) were added and incubated with gels for 30 min at 37 °C. After washing, Alexa Fluor™ 660 C2 Maleimide (ex/em: 650/665 nm) in PBS was then added and incubated for another 30 min at 37 °C. After the incubation, gels were washed with PBS for multiple times, and fluorescent images were taken with an EVOS microscope. Fluorescence intensity were further measured on a plate reader.

2.6. Preparation of gelatin tough hydrogels

30% (w/w) acrylic acid, 10% (w/w) gelatin, 0.3% (w/w) thiolactone acrylamide or (acrylic acid *N*-hydroxysuccinimde ester), 0.1% (w/w) gelMA, and 0.2% (w/w) α-ketoglutaric acid were dissolved in deionized water. The mixture was poured into a PTFE mold and cured in an ultraviolet light chamber (320 nm, 40 W power) for 10 min. For some tests, the gels were completely dried in a 60 °C oven. For all the experiments, gels with a thickness of 250 μm were used unless otherwise mentioned.

2.7. Gel elastic modulus measurement

Thiolactone- or NHS-bearing tough hydrogels with a dimension of 25 mm * 25 mm * 250 μm (W*L*H) were prepared. After fully hydrated with deionized water, gels were placed on the top of a mold with a 15 mm hole. After the gel was firmly clamped onto the mold, a rod with a diameter of 10 mm was used to push down the gel for 12 mm on a mechanical testing machine (Electroforce 3200). The modulus of elasticity can be calculated by following equation:

$$W_{max} = 0.0242\frac{Pa^2}{Eh^3}$$

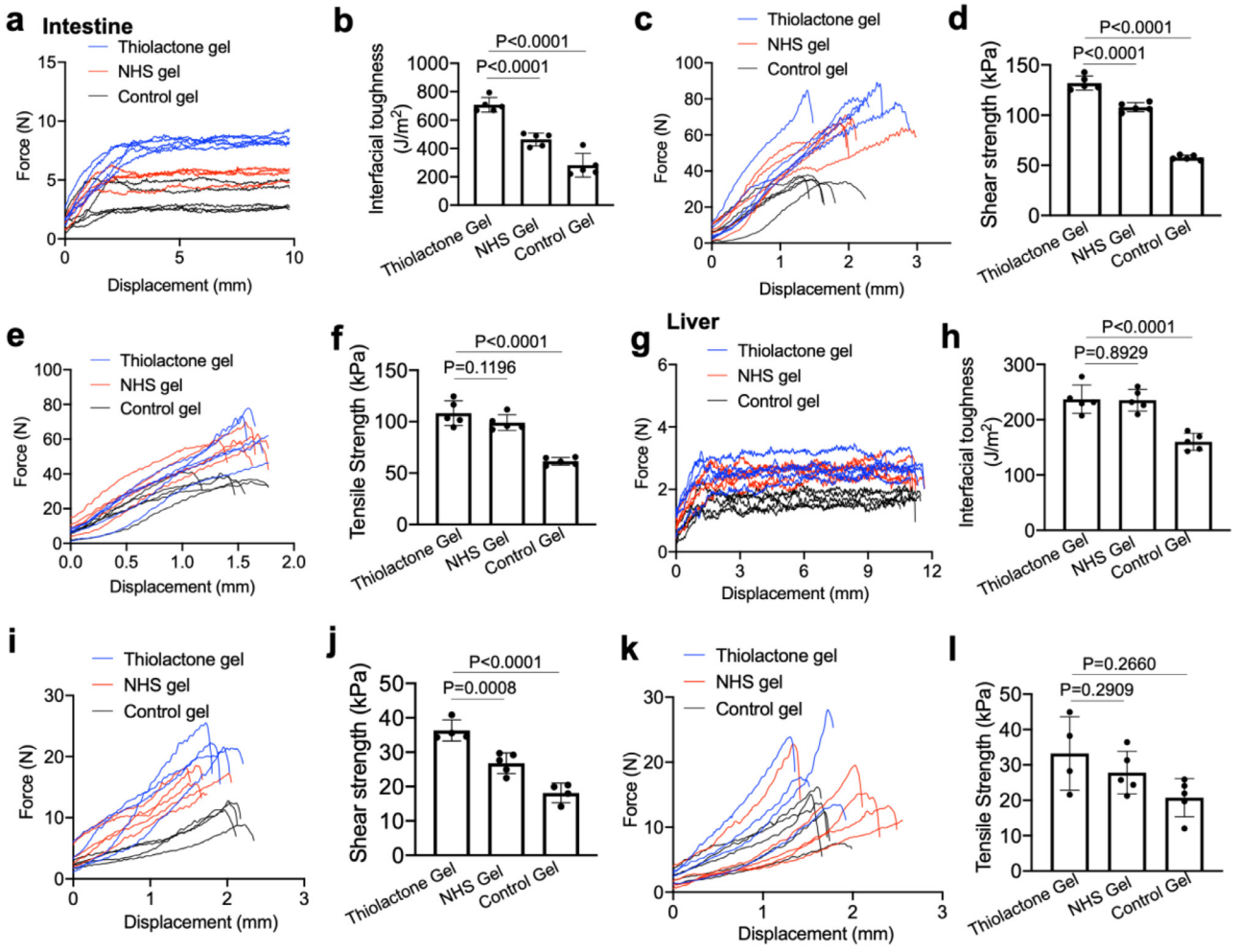

Fig. 6. Thiolactone-bearing tough hydrogels can robustly adhere to various types of tissues. (a) Force-displacement profiles and (b) interfacial toughness of porcine small intestines adhered by thiolactone or NHS or control gels, as determined via a peeling test. (c) Force-displacement profiles and (d) shear strength of porcine small intestines adhered by thiolactone or NHS or control gels, as determined via a lap-shear test. (e) Force-displacement profiles and (f) tensile strength of porcine small intestines adhered by thiolactone or NHS or control gels, as determined via a tensile test. (g) Force-displacement profiles and (h) interfacial toughness of porcine liver adhered by thiolactone or NHS or control gels, as determined via a peeling test. (i) Force-displacement profiles and (j) shear strength of porcine liver adhered by thiolactone or NHS or control gels, as determined via a lap-shear test. (k) Representative force-displacement profiles and (l) tensile strength of porcine liver adhered by thiolactone or NHS or control gels, as determined via a tensile test. (m) Picture showing the adhesion of thiolactone tough gels onto the bleeding mouse heart for rapid hemostasis. All gels tested have a dimension of 24 mm × 24 mm × 0.25 mm. All the numerical data are presented as mean ± SD ($0.01 < {}^{*}P \leq 0.05$; ${}^{**}P \leq 0.01$; ${}^{***}P \leq 0.001$). (For interpretation of the references to colour in this figure legend, the reader is referred to the web version of this article.)

Here, W_{max} is the maximum deflection, P is the pressure applied, a is the diameter of the gel, h is the thickness of the gel, and E is the elastic modulus.

2.8. Preparation of amine-modified engineering solids

Polycarbonate substrates were immersed with the hexamethylenediamine (HMDA) solution (10% (v/v) in deionized water) for 24 h at room temperature to functionalize the surface of polycarbonate sheets with amine groups. After washed with water for five times, polycarbonate sheets were covered with parafilm and stored at room temperature until use.

2.9. Adhesion tests with engineering solids

Amine-functionalized polycarbonate sheets were washed with PBS. Thiolactone- or NHS-bearing tough hydrogels were adhered onto the polycarbonate sheets. 1 kPa pressure was applied for 5 s to ensure the adhesion. Samples were then stored in PBS for 24 h to reach equilibrium swelling of the adhered gel. The gels were soaked but not immersed in PBS in a closed system. PBS is added every few hours to keep the closed system humid. To measure the interfacial toughness of the gel, the samples were tested by a peeling test. L-shaped aluminum fixtures were attached to the polycarbonate sheets by cyanoacrylate glue to guide the peeling test. The specimen was pulled with a constant speed of 50 mm/min by Electromechanical test frame (CRITERION C43.104E Tall Dual Column 10 kN Frame) with a 200 N load cell. The interfacial toughness can be calculated by dividing two times the maximum force measured by the width of the sample. To measure the shear strength, the samples were tested by the standard lab-shear test (ASTM D5868) using an electromechanical test frame with a 200 N load cell. A lap-shear test was conducted with 50 mm/min peeling speed. Shear strength was calculated by dividing the maximum force by the adhesion area. To measure tensile strength, the samples were tested by the standard tensile test (ASTM D897) using an electromechanical test frame with a 200 N load cell. A tensile test was conducted with a 50 mm/min peeling speed. tensile strength was calculated by dividing the maximum force by the adhesion area. Engineering solids were attached to T-shaped aluminum fixtures with cyanoacrylate glue to provide grips for the measurement.

2.10. Adhesion tests with wet tissues

Porcine tissues were stored with an excess of 0.01% (w/v) sodium azide solution to prevent degradation. 50 μm poly(methylmethacrylate) films were attached by cyanoacrylate glue as a backing to prevent the stretching of the tissue. After washing the porcine tissues with PBS, the gelatin tough gel was applied onto the tissue, followed by pressing with 1 kPa pressure for 5 s. Samples then stored in a wet environment for 24 h to reach swelling equilibrium. To measure the interfacial toughness of the gel, the samples were tested by the standard T-peel test (ASTM D1876) using an electromechanical test frame (CRITERION C43.104E Tall Dual Column 10 kN Frame) with a 200 N load cell. The T-peel test was conducted with 50 mm/min peeling speed. The load measured during the peel test reached a plateau as the peeling reached a steady state. After the force was measured by the T-peel test, the interfacial toughness was calculated by dividing two times the plateau force by the width of the tissue sample. Shear strength and tensile strength were measured following the abovementioned procedures.

2.11. In vitro biocompatibility test

Thiolactone-bearing tough hydrogels or NHS-bearing tough hydrogels modified gels were plated in 24-well plates. 3T3-L1 cells were then placed on top of the gels and incubated at 37 °C for 48 h in 5% CO_2. Live and dead cells were stained by 5 µM Calcein AM and Ethidium Homodimer-1, respectively. Fluorescent images were taken with an EVOS microscope.

2.12. In vivo biocompatibility study

C57BL/6 mice were divided into three groups: thiolactone-bearing gels ($n = 5$), NHS-bearing gels ($n = 5$), and no treatment ($n = 5$). Gels were freshly prepared and subcutaneously administered to the flank of C57BL/6 mice on day 0. Weight of mice were closely monitored after the implant. On day 10, gels and lymph nodes were harvested. Harvested tissues were treated with collagenase IV (0.5 mg/mL) for 45 min. After treated with collagenase IV, tissues were disrupted using a syringe plunger to release cells. Cells were collected, washed, and stained for flow cytometry analysis. For the evaluation of overall immune cell populations, cells were stained with FITC-conjugated anti-CD45, PE-conjugated anti-CD11b, PE/Cy7-conjugated anti-CD11c, Alexa Fluor 700-conjugated anti-Ly-6 G/Ly-6C, PerCP/Cy5.5-conjugated anti-F4/80.

2.13. Release of cargo from tough gels

Cargo-encapsulating thiolactone tough gels were fabricated by dissolving Dextran-FITC or DBCO–Cy5 in 1 mL of gelatin mixture (30% (w/w) acrylic acid, 10% (w/w) gelatin, 0.3% (w/w) thiolactone acrylamide, 0.1% (w/w) GelMA, and 0.2% (w/w) α-ketoglutaric acid), and cured in the ultraviolet light chamber (320 nm, 40 W power) for 15 min. Gels were then placed in PBS in a 24-well plate. At selected time points, 100 µL aliquot of supernatants was sampled for quantification of released cargo on a plate reader.

2.14. Blood clotting test

C57BL/6 mouse was euthanized before opening up the chest. The heart was punctured with a 16 G needle to cause bleeding. The gelatin tough gel was quickly applied onto the punctured area.

2.15. Burst pressure test

The burst pressure of the gels was measured according to the ASTM-F2392–04R, Standard Test Method for Burst Strength of Surgical Sealants. As a tissue model, porcine heart was used. 4 mm in diameter hole was made with biopsy punch. PBS were applied to the surface of the tissue to keep the surface wet. To test the burst strength of the gel, porcine hearts were divided into four groups: thiolactone-bearing gels ($n = 5$), NHS-bearing gels ($n = 5$), control gels ($n = 5$), and Dermabond (Medical Mega, New Jersey) ($n = 5$). The gels were applied followed by gently pressing for 5 s with a finger. The porcine heart was then connected to a syringe pump filled with PBS solution. PBS were injected with the speed of 20 mL/min. Digital manometer was connected along the tubes to measure the maximum pressure applied during the pumping.

2.16. Statistical analyses

Statistical analysis was performed using GraphPad Prism v6 and v8. Sample variance was tested using the F test. For samples with equal variance, the significance between the groups was analyzed by a two-tailed student's t-test. For samples with unequal variance, a two-tailed Welch's *t*-test was performed. For multiple comparisons, a one-way analysis of variance (ANOVA) with post hoc Fisher's LSD test was used. The results were deemed significant at $0.01 < {}^{*}P \leq 0.05$, highly significant at $0.001 < {}^{**}P \leq 0.01$, and extremely significant at ${}^{***}P \leq 0.001$.

3. Results and discussion

Prior to the fabrication of tough hydrogels, we first synthesized thiolactone-modified acrylamide, *N*-(2-oxotetrahydrothiophen-3-yl)acrylamide, via the conjugation between $_{D,L}$-DOLOCYSTEINE thiolactone and acryloyl chloride. *N*-(2-oxotetrahydrothiophen-3-yl)acrylamide was well characterized by ^{1}H NMR and ^{13}C NMR spectrometry (Fig. S1–2). To demonstrate the reaction between thiolactone and amine groups, we mixed the synthesized thiolactone acrylamide and hexylamine or dopamine at 1:1 molar ratio in acetonitrile/water (50%/50%, v/v), and monitored the reaction at room temperature via high-performance liquid chromatography (HPLC) (Fig. 2a). At 10 min post mixing, a new peak showed up in HPLC (labeled as compound 2), indicating the successful conjugation between thiolactone and amine groups (Fig. 2b). Allowing for a longer reaction time, thiolactone acrylamide continued to be consumed and more conjugates were formed (Fig. 2b). After mixing the two compounds for over 60 min, another new peak appeared in HPLC (labeled as compound 3), as a result of the crosslinking between thiol groups (Fig. 2b). To further confirm these phenomena, we mixed thiolactone acrylamide with another amine compound, dopamine, at 1:1 molar ratio in acetonitrile/water (50%/50%, v/v) (Fig. 2c). Within 10 min of mixing, a new peak close to the dopamine peak which corresponds to the conjugate (labeled as compound 2) was formed (Fig. 2c). At 140 min, new compounds with less polarity were detected (labeled as compound 3), which correspond to the disulfide compounds resulted from the crosslinking of thiol groups (Fig. 2c). It is noteworthy that these reactions were performed in acetonitrile/water at room temperature, under which condition the conventional Michael addition reaction between thiol and alkene unlikely occurs. These experiments demonstrated the covalent conjugation between thiolactone and amine groups and subsequent crosslinking of the resulting thiols.

We next synthesized thiolactone-bearing tough hydrogels by polymerizing thiolactone acrylamide, GelMA, and acrylic acid in the presence of α-ketoglutaric acid and ultraviolet (UV) irradiation. UV irradiation of α-ketoglutaric acid is supposed to generate free radicals for subsequent co-polymerization of thiolactone acrylamide, GelMA, and acrylic acid. After irradiated with UV light for 10 min, a clear and highly stretchable hydrogel was formed (Fig. 3a). The formed tough gels, even at a very low thickness

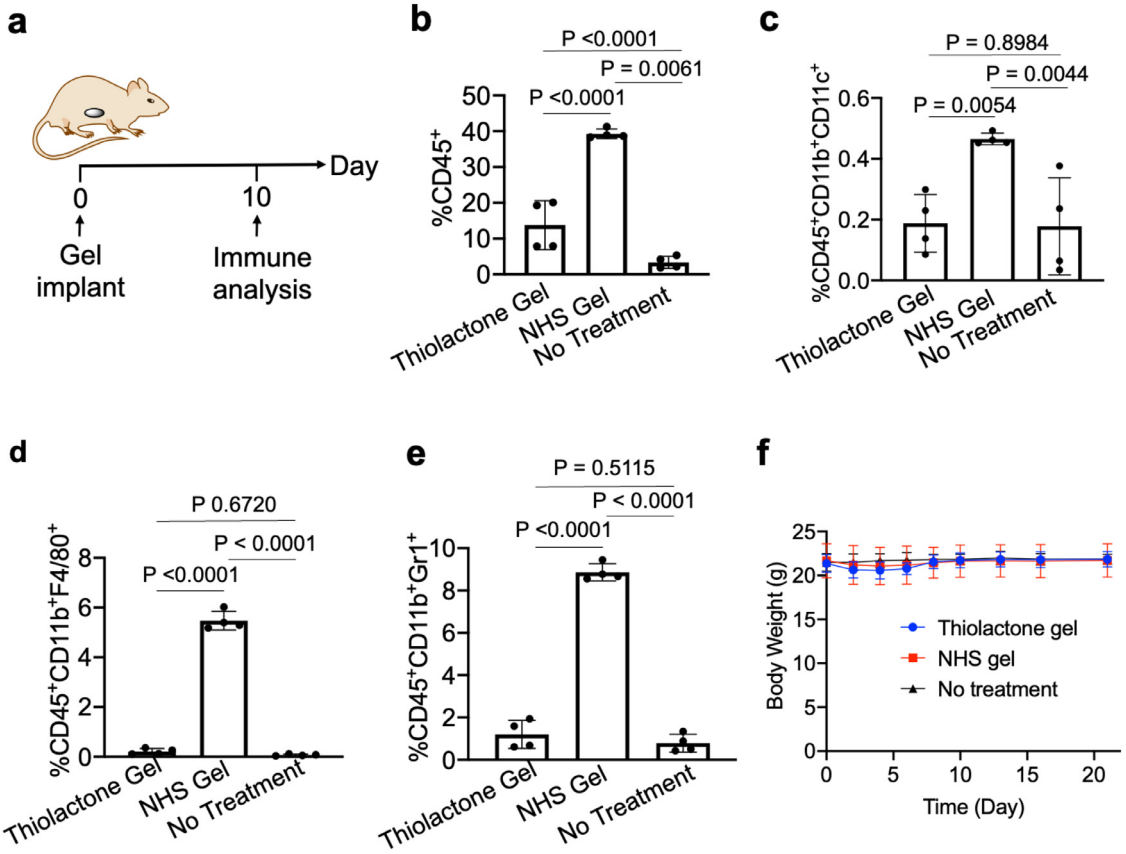

Fig. 7. Thiolactone-bearing tough hydrogels exhibit reduced immunogenicity compared to NHS-bearing gels. (a) Timeframe of animal study. C57BL/6 mice were subcutaneously implanted with gels (attached to the inner side of skin), followed by the analysis of immune cells in gels and surrounding tissues after 10 days. (b) Percentages of $CD45^+$ immune cells in skin tissues surrounding gels or control skin tissues. (c) Percentages of $CD45^+CD11b^+CD11c^+$ dendritic cells in tissues surrounding gels or control tissues. (d) Percentages of $CD45^+CD11b^+F4/80^+$macrophages in tissues surrounding gels or control tissues. (e) Percentages of $CD45^+CD11b^+Gr1^+$ neutrophils in tissues surrounding gels or control tissues. (f) Body weight of mice over the course of a parallel animal study. All the numerical data are presented as mean ± SD ($0.01 < {}^*P \leq 0.05$; ${}^{**}P \leq 0.01$; ${}^{***}P \leq 0.001$). (For interpretation of the references to colour in this figure legend, the reader is referred to the web version of this article.)

(250 μm), can be stretched over 5-fold of initial length without any sign of fracture (Fig. 3a). Mechanical tests of the fabricated gels revealed a high elastic modulus (~1.0 MPa) (Fig. 3b), which indicated the high toughness of the formed gel in comparison with several tens to hundreds of kPa for common gelatin-based hydrogels. As a control, NHS-bearing tough hydrogels were also synthesized using the same method except for the replacement of thiolactone acrylamide with acrylate NHS ester. NHS-bearing hydrogels showed a similar elastic modulus (~1 MPa) to thiolactone-bearing tough hydrogels (Fig. 3b). We next studied the biocompatibility of thiolactone-bearing tough hydrogels. 3T3-L1 fibroblasts were seeded on the hydrogels, and monitored for cell attachment, survival, and proliferation. After 48 h, 3T3-L1 fibroblasts adhered and spread well on the thiolactone-bearing tough hydrogels (Fig. 3c). By staining live cells with Calcein AM and dead cells with Ethidium Homodimer-1 after 48-h culture, 3T3-L1 cells cultured on the thiolactone-bearing tough hydrogels showed a high viability of 98% (Fig. 3c-d). Cells also spread well on the surface of thiolactone-bearing gels, with minimal sign of toxicity (Fig. 3c). In comparison, cells cultured on NHS-bearing tough hydrogels exhibited a lower viability after 48 h, with a higher variation across replicates (Fig. 3d). These experiments demonstrated the great biocompatibility of thiolactone-bearing tough hydrogels.

To further confirm the ability of thiolactone-bearing hydrogels to adhere to amine-modified surface via a two-step mechanism. We first incubated thiolactone-bearing gels, NHS-bearing gels, or control gels with amine-modified fluorescent beads (ex/em: 505/515 nm) for 30 min, and then Alexa Fluor 660 Maleimide (ex/em: 650/665 nm) for another 30 min (Fig. 3e). After washing, the gels were imaged under a fluorescence microscope. Compared to control gels, both thiolactone-bearing gels and NHS-bearing gels successfully captured amine-modified fluorescent beads (Fig. 3f), indicating the covalent conjugation between amine and thiolactone or NHS groups. Thiolactone-bearing tough gels instead of NHS-bearing gels further successfully captured Alexa Fluor 660 Maleimide (Fig. 3f), demonstrating the successful generation of thiol groups in the first step for subsequent conjugation with the maleimide-bearing dye. The measurement of fluorescence intensity via a plate reader also supported the successful capture of amine-modified fluorescent beads and then Alexa Fluor 660 Maleimide by thiolactone-bearing tough gels (Fig. 3g-h).

We next studied the adhesive property of thiolactone- or NHS-bearing tough gels towards amine-modified engineering solids such as polycarbonate. Polycarbonate substrate was modified with amine groups by immersing in a solution of hexamethylenediamine (HMDA, 10% v/v in deionized water) for 24 h (Fig. 4a). After multiple washing steps, thiolactone- or NHS-bearing tough hydrogels were applied to the surface of amine-modified or unmodified polycarbonate (Fig. 4a). By manually peeling the gel from the substrate, a much stronger adhesion was observed towards amine-modified polycarbonate than unmodified polycarbonate for thiolactone-bearing tough gels. The as-synthesized thiolactone- or NHS-bearing tough gels could adhere to amine-modified substrates from both sides, which enabled us to easily perform the peeling,

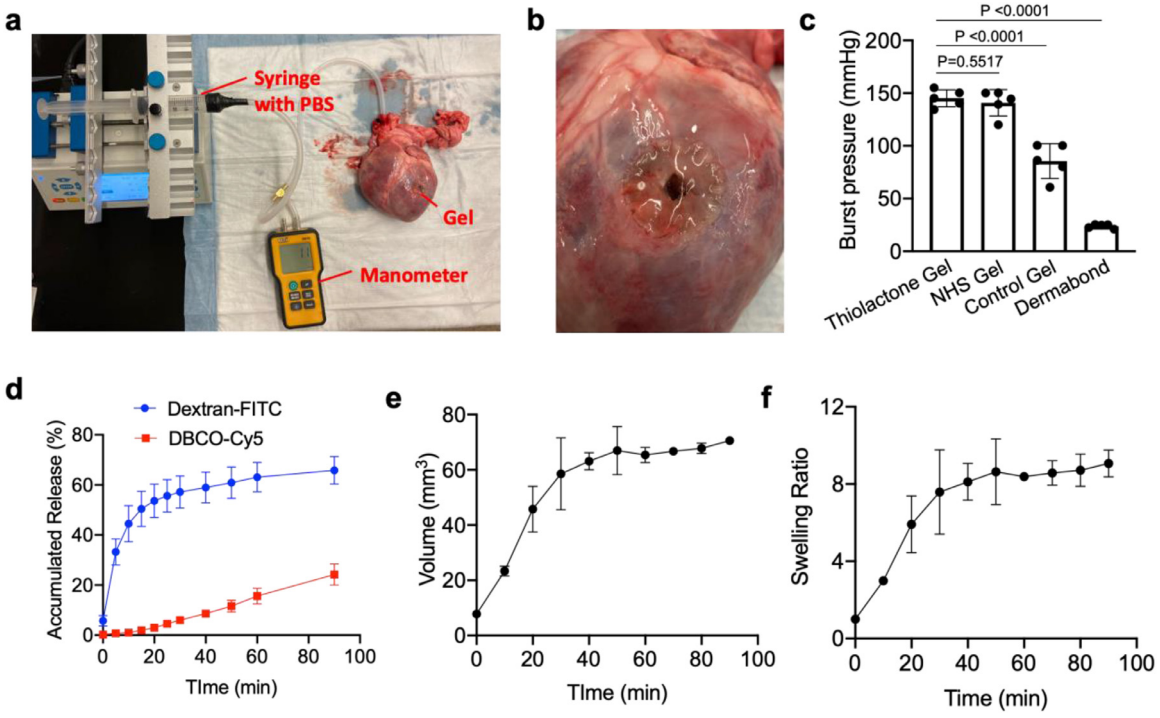

Fig. 8. Thiolactone-bearing tough hydrogels for sealant and drug delivery applications. (a) Experiment set-up of the burst pressure test. (b) Representative picture of thiolactone-bearing gels attached to the punched hole on a porcine liver. (c) Measured burst pressure of thiolactone-bearing gels, NHS gels, control gels, or dermabond (d) Release profiles of dextran-FITC (~40,000 Da) and DBCO–Cy5 (1211.6 Da) from thiolactone-bearing tough hydrogels over time. (e) Volume change of thiolactone-bearing tough gels over time after immersed in PBS at 37 °C. (f) Swelling ratio of thiolactone-bearing tough gels over time after immersed in PBS at 37 °C. All the numerical data are presented as mean ± SD. (For interpretation of the references to colour in this figure legend, the reader is referred to the web version of this article.)

lap-shear, and tensile tests for adhesion measurements (Fig. S3–5). We first performed a peeling test by placing the thiolactone-bearing tough hydrogel between two amine-modified polycarbonate substrates, applying 1 kPa pressure for 5 s to ensure the adhesion, and then storing the samples in PBS for 24 h to allow the gels to swell and equilibrate. It is noteworthy that a good adhesion between gels and polycarbonate substances was already formed after applying the pressure. Polycarbonate substrates with gels in between were then fixed to the horizontal lever of the testing machine (Fig. 4b, Fig. S3). Thiolactone-bearing tough gels exhibited an adhesion energy of ~870 J/m^2 towards amine-modified polycarbonate, which is significantly higher than the control group (~390 J/m^2) (Fig. 4c), demonstrating the strong adhesion of thiolactone-bearing tough gels to amine-modified engineering solids. NHS-bearing tough gels also showed a high adhesion energy (~700 J/m^2), albeit lower than thiolactone-bearing tough gels (Fig. 4c). To further validate the adhesion of thiolactone-bearing tough gels, we also performed the lap-shear and tensile tests using the amine-modified polycarbonate substrates (Fig. S4–5). Thiolactone-bearing tough hydrogels resulted in a shear strength of ~90 kPa and a tensile strength of ~67 kPa (Fig. 4d-e, Fig. S4–5), in comparison with ~50 kPa shear strength and ~67 kPa tensile strength for NHS-bearing tough hydrogels.

After demonstrating the ability of thiolactone-bearing tough hydrogels to strongly adhere to amine-modified engineering solids, we next studied their adhesion towards wet tissues. Similar to the amine-modified engineering solids, thiolactone-bearing tough hydrogels could also easily adhere to porcine skin (Fig. 5a). Two pieces of porcine skin could be strongly adhered together by the thiolactone-bearing tough gel (24 × 24 × 0.25 mm), for the quantification of adhesion energy (or interfacial toughness) (Fig. 5a, Fig. S6). Thiolactone-bearing tough gels showed an adhesion energy of ~920 J/m^2 towards porcine skin, which is significantly higher than that of NHS-bearing gels (~750 J/m^2) (Fig. 5b-c). Both thiolactone- and NHS-bearing gels exhibited a significantly higher adhesion energy than control gels without thiolactone or NHS groups (Fig. 5b-c), demonstrating the importance of covalent linkages between gels and tissues. The shear strength and tensile strength of porcine skin adhered by gels were also measured via lap-shear and tensile tests, respectively, with a shear strength of 137 kPa and tensile strength of 81 kPa for thiolactone-bearing tough gels (Fig. 5d-g, Fig. S6). Compared to NHS-bearing gels, thiolactone-bearing tough hydrogels resulted in a slightly higher shear strength and a similar tensile strength (Fig. 5d-g). The shear strength and tensile strength resulted from thiolactone-bearing tough gels were significantly higher than control gels without covalent linkages with the tissue (Fig. 5d-g). It is noteworthy that the adhesion energy of thiolactone-bearing tough hydrogels is much higher than commercial bioadhesives including Dermabond, Tissel, and Duraseal, which are all below 250 J/m^2 (Fig. 5h) [3,6].

We also characterized the adhesion of thiolactone-bearing tough gels towards porcine small intestine and liver. Similar to porcine skin, thiolactone-bearing tough gels resulted in a higher adhesion energy towards small intestine compared to NHS-bearing gels or control gels (Fig. 6a-b). The shear strength of thiolactone-bearing gel adhesives was also higher than that of NHS-bearing gel adhesives (Fig. 6c-d), albeit showing a similar tensile strength (Fig. 6e-f). Both thiolactone- and NHS-bearing gels showed a significantly higher shear strength and tensile strength than control gels (Fig. 6c-f). Different from skin and small intestine, the adhesion of thiolactone-bearing tough gels towards porcine liver was relatively weak, with an adhesion energy of 237 J/m^2 (Fig. 6g-h). Nevertheless, thiolactone-bearing gels still exhibited much higher adhesion energy and shear strength in comparison with the control

gels (Fig. 6g-l). These experiments well demonstrated the superior adhesive property of thiolactone-bearing tough hydrogels towards different types of tissues, presumably due to the two-step crosslinking/adhesion mechanism.

We next studied and compared the immunogenicity of thiolactone-bearing gels and NHS-bearing gels. Immunocompetent C57BL/6 mice were subcutaneously implanted with gels (attached to the inner side of skin), followed by the analysis of immune cells in gels and surrounding tissues after 10 days (Fig. 7a). Strikingly, NHS-bearing tough gels induced the recruitment of a significantly higher number of $CD45^+$ immune cells, in comparison with thiolactone-bearing tough gels or untreated tissues (Fig. 7b). Similarly, a much higher number of $CD11b^+CD11c^+$ dendritic cells (Fig. 7c), $CD11b^+F4/80^+$ macrophages (Fig. 7d), and $CD11b^+Gr1^+$ neutrophils (Fig. 7e) were detected in tissues surrounding NHS-bearing gels than thiolactone-bearing gels. Compared to the untreated tissues, tissues surrounding thiolactone-bearing gels contained a higher number of $CD45^+$ immune cells but showed negligible differences in the number of dendritic cells, macrophages, and neutrophils (Fig. 7b-e). These data demonstrated the significantly higher immunogenicity of NHS-bearing gels than thiolactone-bearing gels, supporting our hypothesis that thiolactone-bearing gels based on the side product-free thiolactone-amine chemistry could show improved biocompatibility.

We envision various applications of the thiolactone-bearing tough gel adhesive including hemostasis, drug delivery, tissue repair, and mechanotherapy. As a proof-of-concept demonstration for sealant application, we performed a burst pressure test with porcine heart (Fig. 8a). After punching the porcine heart with a hole of 4 mm in diameter, thiolactone-bearing gel or NHS-bearing gel or control gel or Dermabond was applied to the punched area (Fig. 8b), followed by the measurement of burst pressure upon injection of PBS (Fig. 8a). Compared to the control gel or Dermabond, both thiolactone-bearing tough gels or NHS-bearing tough gels resulted in significantly higher burst pressure (Fig. 8c), demonstrating their stronger sealant effect. As a quick test for hemostatic applications, we also showed that thiolactone tough gels could easily and rapidly adhere to the bleeding mouse heart for hemostasis (Fig. S7). After demonstrating that thiolactone-bearing tough hydrogels can robustly adhere to engineering solids and wet tissues, we next studied their potential as a depot for drug delivery. Two model fluorescent compounds of different molecular weights and hydrophilicity, dextran-FITC (~40,000 Da) and dibenzocyclooctyne (DBCO)-Cy5 (1211.6 Da), were encapsulated into the tough hydrogels by mixing them with the monomers and crosslinkers prior to polymerization. Surprisingly, dextran-FITC with a much higher molecular weight than DBCO–Cy5 showed significantly faster release from thiolactone-bearing tough hydrogels, with ~66% of loaded dextran-FITC released within 90 min (Fig. 8d). In contrast, ~24% of encapsulated DBCO–Cy5 was released from the gels within 90 min (Fig. 8d). The significantly higher release rate of higher-molecular-weight dextran-FITC is inconsistent with the typical phenomena observed with hydrogel-based drug delivery systems, but could be potentially explained by the higher hydrophilicity of dextran-FITC than DBCO–Cy5, especially considering the high water-adsorbing capability of the tough hydrogel. In support of this, thiolactone-bearing tough hydrogels showed rapid swelling when cultured at 37 °C (Fig. 8e), with a swelling ratio of ~7.6 within 30 min (Fig. 8f). The high amount of water diffusing into the tough hydrogels and the exchange of water molecules between the hydrogels and the surrounding culture medium likely accounted for the rapid release of hydrophilic dextran-FITC. These experiments demonstrated that thiolactone-bearing tough hydrogels not only can strongly adhere to various types of tissues, but can also function as a drug depot for local release of drugs of different molecular weights. The ability to release cargos while strongly adhering to tissues holds great promise for tissue repair and drug delivery applications.

4. Conclusion

To summarize, we report the use of side product-free thiolactone-amine chemistry, which initiates a double crosslinking adhesion mechanism, for the development of tough hydrogel adhesives. The thiolactone-bearing tough hydrogels showed high mechanical strength, good biocompatibility, and robust adhesion to both engineering solids and wet tissues (porcine skin, small intestine, and liver). In addition to functioning as an adhesive and hemostatic sealant, thiolactone-bearing tough hydrogels also enabled controlled release of cargos of different molecular weights. We envision various promising applications of thiolactone-bearing tough gel adhesives including hemostasis, tissue repair, mechanotherapy, and drug delivery. The success of thiolactone-amine chemistry to mediate strong adhesion to wet tissues also expands the currently-minimal library of available covalent chemistries for tissue adhesion, and will greatly facilitate future development of bioadhesive systems.

Data availability

Raw data can be accessed upon request, and will be published upon the acceptance of the manuscript.

Declaration of Competing Interest

The authors declare no competing financial interests.

Acknowledgements

The authors would like to acknowledge the financial support from NSF DMR 21–43673 CAR and the start-up package from the Department of Materials Science and Engineering at the University of Illinois at Urbana-Champaign and the Cancer Center at Illinois.

Supplementary materials

Supplementary material associated with this article can be found, in the online version, at doi:10.1016/j.actbio.2022.07.028.

References

[1] B. Xue, J. Gu, L. Li, W. Yu, S. Yin, M. Qin, Q. Jiang, W. Wang, Y. Cao, Hydrogel tapes for fault-tolerant strong wet adhesion, Nat. Commun. 12 (1) (2021) 1–12.
[2] H. Yuk, J. Wu, T.L. Sarrafian, X. Mao, C.E. Varela, E.T. Roche, L.G. Griffiths, C.S. Nabzdyk, X. Zhao, Rapid and coagulation-independent haemostatic sealing by a paste inspired by barnacle glue, Nature Biomed. Eng. 5 (10) (2021) 1131–1142.
[3] J. Li, A. Celiz, J. Yang, Q. Yang, I. Wamala, W. Whyte, B. Seo, N. Vasilyev, J. Vlassak, Z. Suo, Tough adhesives for diverse wet surfaces, Science 357 (6349) (2017) 378–381.
[4] H. Jung, M.K. Kim, J.Y. Lee, S.W. Choi, J. Kim, Adhesive hydrogel patch with enhanced strength and adhesiveness to skin for transdermal drug delivery, Adv. Funct. Mater. 30 (42) (2020) 2004407.
[5] A.K. Geim, S. Dubonos, I. Grigorieva, K. Novoselov, A. Zhukov, S.Y. Shapoval, Microfabricated adhesive mimicking gecko foot-hair, Nat. Mater. 2 (7) (2003) 461–463.
[6] H. Yuk, C.E. Varela, C.S. Nabzdyk, X. Mao, R.F. Padera, E.T. Roche, X. Zhao, Dry double-sided tape for adhesion of wet tissues and devices, Nature 575 (7781) (2019) 169–174.
[7] Y. Zhang, S. Li, P. Zuo, J. Ji, J. Liu, The mechanics of abalone crawling on sharp objects without injury, Sci. Rep. 9 (1) (2019) 1–7.
[8] V. Bhagat, M.L. Becker, Degradable adhesives for surgery and tissue engineering, Biomacromolecules 18 (10) (2017) 3009–3039.
[9] D. Zhang, J. Liu, Q. Chen, W. Jiang, Y. Wang, J. Xie, K. Ma, C. Shi, H. Zhang, M. Chen, A sandcastle worm-inspired strategy to functionalize wet hydrogels, Nat. Commun. 12 (1) (2021) 1–14.
[10] Y. Zhang, S. Li, P. Zuo, J. Li, J. Liu, A Mechanics Study on the Self-Righting of Abalone from the Substrate, Appl. Bionics Biomech. 2020 (2020).

[11] S. Blacklow, J. Li, B. Freedman, M. Zeidi, C. Chen, D. Mooney, Bioinspired mechanically active adhesive dressings to accelerate wound closure, Sci. Adv. 5 (7) (2019) eaaw3963.
[12] J.-.Y. Sun, X. Zhao, W.R. Illeperuma, O. Chaudhuri, K.H. Oh, D.J. Mooney, J.J. Vlassak, Z. Suo, Highly stretchable and tough hydrogels, Nature 489 (7414) (2012) 133–136.
[13] M.A. Haque, T. Kurokawa, J.P. Gong, Super tough double network hydrogels and their application as biomaterials, Polymer (Guildf) 53 (9) (2012) 1805–1822.
[14] T. Matsuda, T. Nakajima, J.P. Gong, Fabrication of tough and stretchable hybrid double-network elastomers using ionic dissociation of polyelectrolyte in non-aqueous media, Chem. Mater. 31 (10) (2019) 3766–3776.
[15] B.R. Freedman, O. Uzun, N.M.M. Luna, A. Rock, C. Clifford, E. Stoler, G. Östlund-Sholars, C. Johnson, D.J. Mooney, Degradable and Removable Tough Adhesive Hydrogels, Adv. Mater. 33 (17) (2021) 2008553.
[16] L.K. Borden, A. Gargava, S.R. Raghavan, Reversible electroadhesion of hydrogels to animal tissues for suture-less repair of cuts or tears, Nat. Commun. 12 (1) (2021) 1–10.
[17] S.J. Frost, D. Mawad, M.J. Higgins, H. Ruprai, R. Kuchel, R.D. Tilley, S. Myers, J.M. Hook, A. Lauto, Gecko-inspired chitosan adhesive for tissue repair, NPG Asia Mater. 8 (6) (2016) e280 -e280.
[18] J. Woodley, Bioadhesion, Clin. Pharmacokinet. 40 (2) (2001) 77–84.
[19] M. Mehdizadeh, J. Yang, Design strategies and applications of tissue bioadhesives, Macromol. Biosci. 13 (3) (2013) 271–288.
[20] D. Zhou, S. Li, M. Pei, H. Yang, S. Gu, Y. Tao, D. Ye, Y. Zhou, W. Xu, P. Xiao, Dopamine-modified hyaluronic acid hydrogel adhesives with fast-forming and high tissue adhesion, ACS Appl. Mater. Interfaces 12 (16) (2020) 18225–18234.
[21] Y. Hong, F. Zhou, Y. Hua, X. Zhang, C. Ni, D. Pan, Y. Zhang, D. Jiang, L. Yang, Q. Lin, A strongly adhesive hemostatic hydrogel for the repair of arterial and heart bleeds, Nat. Commun. 10 (1) (2019) 1–11.
[22] Y. Hua, H. Xia, L. Jia, J. Zhao, D. Zhao, X. Yan, Y. Zhang, S. Tang, G. Zhou, L. Zhu, Ultrafast, tough, and adhesive hydrogel based on hybrid photocrosslinking for articular cartilage repair in water-filled arthroscopy, Sci. Adv. 7 (35) (2021) eabg0628.
[23] N. Lang, M.J. Pereira, Y. Lee, I. Friehs, N.V. Vasilyev, E.N. Feins, K. Ablasser, E.D. O'Cearbhaill, C. Xu, A. Fabozzo, A blood-resistant surgical glue for minimally invasive repair of vessels and heart defects, Sci. Transl. Med. 6 (218) (2014) 218ra6 -218ra6.
[24] Y. Wang, K. Jia, C. Xiang, J. Yang, X. Yao, Z. Suo, Instant, tough, noncovalent adhesion, ACS Appl. Mater. Interfaces 11 (43) (2019) 40749–40757.
[25] L. Ge, S. Chen, Recent advances in tissue adhesives for clinical medicine, Polymers (Basel) 12 (4) (2020) 939.
[26] G.M. Taboada, K. Yang, M.J. Pereira, S.S. Liu, Y. Hu, J.M. Karp, N. Artzi, Y. Lee, Overcoming the translational barriers of tissue adhesives, Nat. Rev. Mater. 5 (4) (2020) 310–329.
[27] Y. Gao, J. Chen, X. Han, Y. Pan, P. Wang, T. Wang, T. Lu, A universal strategy for tough adhesion of wet soft material, Adv. Funct. Mater. 30 (36) (2020) 2003207.
[28] X. Fan, Y. Fang, W. Zhou, L. Yan, Y. Xu, H. Zhu, H. Liu, Mussel foot protein inspired tough tissue-selective underwater adhesive hydrogel, Mater. Horiz. 8 (3) (2021) 997–1007.
[29] M.C. Arno, Engineering the mammalian cell surface with synthetic polymers: strategies and applications, Macromol. Rapid Commun. 41 (18) (2020) 2000302.
[30] S. Nam, D. Mooney, Polymeric tissue adhesives, Chem. Rev. (2021).
[31] A. Sadiki, E.M. Kercher, H. Lu, R.T. Lang, B.Q. Spring, Z.S. Zhou, Site-specific bioconjugation and convergent click chemistry enhances antibody–chromophore conjugate binding efficiency, Photochem. Photobiol. 96 (3) (2020) 596–603.
[32] S. Roy, J.N. Cha, A.P. Goodwin, Nongenetic bioconjugation strategies for modifying cell membranes and membrane proteins: a review, Bioconjug. Chem. 31 (11) (2020) 2465–2475.
[33] P.J. Bouten, M. Zonjee, J. Bender, S.T. Yauw, H. van Goor, J.C. van Hest, R. Hoogenboom, The chemistry of tissue adhesive materials, Prog. Polym. Sci. 39 (7) (2014) 1375–1405.
[34] Z. Ma, G. Bao, J. Li, Multifaceted design and emerging applications of tissue adhesives, Adv. Mater. (2021) 2007663.
[35] J. Deng, H. Yuk, J. Wu, C.E. Varela, X. Chen, E.T. Roche, C.F. Guo, X. Zhao, Electrical bioadhesive interface for bioelectronics, Nat. Mater. 20 (2) (2021) 229–236.
[36] P. Espeel, F.E. Du Prez, One-pot multi-step reactions based on thiolactone chemistry: a powerful synthetic tool in polymer science, Eur. Polym. J. 62 (2015) 247–272.
[37] M. Langlais, O. Coutelier, M. Destarac, Thiolactone-functional reversible deactivation radical polymerization agents for advanced macromolecular engineering, Macromolecules 51 (11) (2018) 4315–4324.
[38] S. Mommer, K.-.N. Truong, H. Keul, M. Möller, An epoxy thiolactone on stage: four component reactions, synthesis of poly(thioether urethane)s and the respective hydrogels, Polym. Chem. 7 (12) (2016) 2291–2298.
[39] J. Li, D.J. Mooney, Designing hydrogels for controlled drug delivery, Nat. Rev. Mater. 1 (12) (2016) 1–17.
[40] C. Cui, T. Wu, X. Chen, Y. Liu, Y. Li, Z. Xu, C. Fan, W. Liu, A Janus hydrogel wet adhesive for internal tissue repair and anti-postoperative adhesion, Adv. Funct. Mater. 30 (49) (2020) 2005689.
[41] S. Tarafder, G.Y. Park, J. Felix, C.H. Lee, Bioadhesives for musculoskeletal tissue regeneration, Acta Biomater. (2020).